International Journal of Pharmaceutics: X 7 (2024) 100258

Contents lists available at ScienceDirect

International Journal of Pharmaceutics: X

journal homepage: www.sciencedirect.com/journal/international-journal-of-pharmaceutics-x

Research on the loading and release kinetics of the vincristine sulfate liposomes and its anti-breast cancer activity

Zixu Liu [a,1], Yang Liu [c,1], Zixuan Wu [a], Boyuan Liu [a], Linxuan Zhao [d], Tian Yin [e], Yu Zhang [a], Haibing He [a], Jingxin Gou [a], Xing Tang [a,*], Song Gao [b,*]

[a] Department of Pharmaceutics Science, Shenyang Pharmaceutical University, Shenyang 110116, China
[b] Department of Oncology, Shengjing Hospital of China Medical University, 39 Huaxiang Road, Shenyang, China
[c] Innovative Research Center for Integrated Cancer Omics, Shengjing Hospital of China Medical University, Shenyang, China
[d] Department of Pharmaceutics, College of Pharmacy Sciences, Jilin University, Changchun 130021, China
[e] Department of Functional Food and Wine, Shenyang Pharmaceutical University, Shenyang 110116, China

ARTICLE INFO

Keywords:
Vincristine sulfate
Liposomes
Drug-loading kinetics
Release kinetics
Cancer treatment

ABSTRACT

Vincristine (VCR), as a cytotoxic drug, is used clinically to treat acute lymphatic leukemia and breast cancer, and commonly used clinically as vincristine sulfate (VCRS). However, its clinical use is limited by unpredictable pharmacologic characteristics, a narrow therapeutic index, and neurotoxicity. The pH gradient method was used for active drug loading of VCRS, and the process route mainly includes the preparation of blank liposomes and drug-loaded liposomes. VCRS liposomes had suitable particle size, high encapsulation efficiency and good stability. The loading and release kinetics of VCRS liposomes were explored. By calculating the changes of encapsulation efficiency with time at different temperatures, it was confirmed that the drug-loading process of liposomes exhibited a first-order kinetic feature, and the activation energy required for the reaction was determined as 20.6 kcal/mol. The release behavior at different pH was also investigated, and it was demonstrated that the release behavior conformed to the first-order model, suggesting that the release mechanism of VCRS was simple transmembrane diffusion. VCRS liposomes also enhanced *in vitro* and *in vivo* antitumor activity. Thus, VCRS liposomes showed great potential for VCRS delivery, and the loading and release kinetics were well researched to provide a reference for investigating active drug loading liposomes.

1. Introduction

Vincristine (VCR) is a vinca alkaloid, unstable, and commonly used clinically as vincristine sulfate (VCRS)(Moore and Pinkerton, 2009). It has a high affinity for microtubule proteins and can inhibit the polymerization of microtubule proteins in tumor cells, hindering the mitotic activity of cells and causing nuclear consolidation and nuclear collapse (Becker et al., 2020; Harmon et al., 1992; Jordan et al., 1985). In addition, it affects the immune cells of the body(Fujimura et al., 2018), can activate adaptive immunity by inducing DNA damage, promoting cytotoxic T lymphocytes (CTLs) infiltration into tumor sites, and enhancing the antitumor immune response(Harding et al., 2017; Serpico et al., 2020). VCR is used clinically for the treatment of acute lymphatic leukemia, breast cancer, malignant lymphoma, small cell lung cancer and pediatric solid tumors(Davis and Farag, 2013), and can also be used in combination with chemotherapy(Hagemeister et al., 2013).

Although VCR is a potent antineoplastic, its clinical use is limited by unpredictable pharmacologic characteristics (*e.g.*, volume of distribution, half-life, and clearance), a narrow therapeutic index, and neurotoxicity(Douer, 2016). By interfering with the assembly and disassembly of microtubule proteins, VCR causes swelling of myelinated fibers and axons of myelinated fibers, which in turn damages nerve fibers(Kavcic et al., 2017). VCR-induced neurotoxicity is mainly manifested in three aspects: peripheral neurotoxicity, cranial neurotoxicity and autonomic neurotoxicity(Nazir et al., 2017). Therefore, the clinical dose is 1.4–1.6 mg/m^2, and the maximum dose should not exceed 2 mg/m^2 (Li et al., 2020).

In order to prolong the *in vivo* circulation of VCRS, reduce the side effects and improve antitumor activity, several preparations have been proposed. Until now, VCRS have been successfully prepared as

* Corresponding authors.
E-mail addresses: tanglab@126.com (X. Tang), gaogao0229@hotmail.com (S. Gao).
[1] Zixu Liu and Yang Liu contributed equally to this work.

https://doi.org/10.1016/j.ijpx.2024.100258
Received 6 April 2024; Received in revised form 28 May 2024; Accepted 30 May 2024
Available online 31 May 2024

nanoparticles, lipid nanoparticles, emulsions, microspheres and liposomes(Chen et al., 2011; Mojarad-Jabali et al., 2022; Naseer et al., 2022). Liposomes stood out from the crowd of carriers due to their high safety, stability, and enhanced tumor-targeting ability, and ultimately achieved approval for marketing(Huwyler et al., 2008; Silverman and Deitcher, 2013). Liposomes are mainly composed of phospholipids and cholesterol, and their structure is a vesicle structure consisting of one or more curved phospholipid bilayers internally encapsulated with an aqueous core(Bangham et al., 1965). The aqueous phase inside the liposomes can encapsulate hydrophilic drugs, and the lipid bilayer can encapsulate hydrophobic drugs(Pauli et al., 2019; Torchilin, 2005). Liposomes, as the drug delivery systems, show numerous advantages, *e.g.*, high drug loading ability, targeting capability, improved drug stability, high biocompatibility, increased drug potency, as well as reduced toxicity(Liu et al., 2022; Monteiro et al., 2014).

The drug loading methods of liposomes are divided into two main categories: passive drug loading and active drug loading. Active drug loading is the establishment of gradient, mainly an ionic gradient and a pH gradient, inside and outside the phospholipid bilayers to drive the drug across the lipid membrane into the liposomes. This method results in higher encapsulation efficiency due to the additional provision of drug loading power. Due to the good amphiphilicity of VCRS, the drug loading method is suitable for active drug loading. With pH gradient drug loading, the drug in liposomes is mostly in solution form, while with anionic gradient, VCRS is mostly in precipitated form. And it has been proven that the VCRS liposomes in precipitated form in the internal aqueous phase are too slow to be released after uptake by the tumor cells, resulting in undesirable therapeutic effect(Noble et al., 2009; Oto et al., 1996), so the pH gradient method is used for drug loading.

Marqibo®, is a proprietary sphingomyelin- and cholesterol-based nanoparticle formulation of VCRS(Wang et al., 2015). Marqibo® is a three-vial combination of VCRS solution, blank liposomes and pH adjuster, which is to be prepared ready to use. The method of use is to draw blank liposomes and VCRS solution in turn, inject into sodium phosphate solution, incubate at 63–67 °C for 10–15 min(Pathak et al., 2014). The liposomes are specifically designed to facilitate the loading and retention of VCRS, prolong the circulation time of encapsulated VCRS, increase extravasation into tumors and slowly release the drug in the tumor interstitium. These characteristics result in high levels of encapsulated drug in target tissues, leading to enhanced antitumor activity(Johnston et al., 2006; Zhigaltsev et al., 2005). However, the emergence of new treatment options (such as targeted drugs) makes it difficult to recruit patients for validation trials. Due to the lack of conclusive evidence of clinical benefit, Acrotech voluntarily withdrawn approval for the indication of Marqibo®.

Based on Marqibo®, we prepared VCRS liposomes. The blank liposomes were prepared by thin film hydration-freeze-thaw extrusion method. The drug-loading process involved mixing and incubating the drug solution, blank liposomes with the pH-adjusting solution. The prescription and process were examined to determine the optimal prescription and process route for VCRS liposomes. The characterization and stability of VCRS liposomes were detected. The loading and release kinetics of VCRS liposomes were explored. The drug-loading process of liposomes exhibited a first-order kinetic feature, and the activation energy required for the reaction was determined as 20.6 kcal/mol. The release behavior conformed to the first-order model by fitting the cumulative release *versus* time curves, suggesting that the release mechanism of the drug was simple transmembrane diffusion. VCRS liposomes also enhanced *in vitro* and *in vivo* antitumor activity. Thus, VCRS liposomes showed great potential for VCRS delivery, and the loading and release kinetics were well researched to play foundation for better explore liposomes.

2. Materials and methods

2.1. Materials

Vincristine sulfate was provided by Baiyunshan Hanfang Modern Pharmaceutical Co., Ltd. (Guangzhou, China). Egg sphingomyelin (ESM), egg yolk lecithin E80, soy lecithin S100 and cholesterol originated from AVT (Shanghai) Pharmaceutical Tech Co., Ltd. Dalian Meilun Biotechnology Co, Ltd. offered the materials about cell culture, including fetal bovine serum (FBS), Roswell Park Memorial Institute 1640 (RPMI 1640), Cell Counting Kit-8 assay.

2.2. Preparation of VCRS liposomes

The prescription and process were optimized based on the patent of Marqibo®(Sarris et al., 2011; Webb et al., 1996).

2.2.1. Preparation of blank liposomes

ESM and cholesterol (2.5:1, w) were dissolved in chloroform. Chloroform was evaporated at 40 °C while lipid films were prepared. Citrate solution (300 mM) was used as the hydration medium, and the films were hydrated under magnetic stirring at 65 °C for 30 min to obtain large-size multilayer liposomes. The obtained large particle size liposomes were subjected to probe sonication. Freeze-thaw cycles (−80 °C ~ 65 °C) were performed five times to initially reduce particle size. Then the liposomes were extruded using a liposome extruder to pass through 200 nm and 100 nm polycarbonate membranes three times at 65 °C. Blank liposomes with rounded morphology and uniform size were obtained, cooled, and stored at 4 °C.

2.2.2. Preparation of VCRS-loaded liposomes

Blank liposomes and VCRS solutions were sequentially withdrawn and placed in sodium phosphate solution (1:5:25, v), magnetically stirred, and incubated in a water bath at 65 °C for 10 min and cooled to room temperature. Then VCRS liposomes were stored at 4 °C.

2.3. Characterization of VCRS liposomes

The particle size, polydispersity index (PDI) value and Zeta potential of blank liposomes and VCRS liposomes were determined using a ZetaSizer (Nano-ZS ZEN3700, Malvern, UK). The morphology was characterized using transmission electron microscope (TEM, JEOL JEM-2000EX) and atomic force microscopy (AFM, Cypher ES, Asylum Research)(Liu et al., 2021b) The content of ESM (Fig.S1) and VCRS (Fig. S2) was quantified using high-performance liquid chromatography (HPLC, Hitachi, Japan). The content of ESM was determined employing a C18 column (5 μm, 250 × 4.6 mm, Diamond). The mobile phase constituted methanol, with the eluents monitored at 202 nm. The content of VCRS was determined employing a C18 column, the mobile phase constituted methanol: 1.5% diethylamine solution (70/30, v), with the eluents monitored at 298 nm. Moreover, the encapsulation efficiency (EE%) of liposomes was detected with the use of the microcolumn centrifugation method(Liu et al., 2022).

2.4. Stability

The VCRS solution and blank liposomes were stored at 4 °C for 6 months and 25 °C for 3 months. At pre-determined time intervals, the VCRS liposomes were prepared, the particle size, drug content and EE% were monitored to evaluate the stability. Rat plasma was taken and diluted with saline to a concentration of 50%. VCRS liposomes were added to 50% plasma samples in different ratios of 1:9 and 2:8 (v), respectively, and placed in a 37 °C water bath with vibration. The particle size was determined at 0, 2, 4, 8, 12, 24, 48 and 72 h, respectively. In addition, the content of VCRS in plasma was determined using HPLC. The VCRS liposomes were diluted 1-fold, 2-fold and 4-fold with saline,

respectively, and incubated at room temperature for 2 h. Samples were taken to determine the EE% and particle size to examine the dilution stability.

2.5. Establishment of drug loading gradient in VCRS liposomes

In this experiment, the pH gradient method was chosen for active drug loading. The establishment of pH gradient method has an important relationship with the proportion of molecular forms of VCR in aqueous solution, so the proportion of various forms of VCR should be quantitatively analyzed according to the acid-base theory. VCR is an organic tetracyclic hetero compound with two tertiary amino groups, which can exist in an aqueous solution in three forms, respectively [VCR], [VCR^+], and [VCR^{2+}]. In order to investigate the proportion δ% of each form as a function of pH, it was calculated according to the following equation:

$$VCR^{2+} \leftrightarrow H^+ + VCR^+$$

$$Ka_1 = \frac{[H^+]\ \delta_{VCR^+}}{\delta_{VCR^{2+}}}$$

$$VCR^+ \leftrightarrow H^+ + VCR$$

$$Ka_2 = \frac{[H^+]\ \delta_{VCR}}{\delta_{VCR^+}}$$

$$\delta_{VCR^{2+}} = \frac{[H^+]^2}{[H^+]^2 + [H^+][Ka_1] + [Ka_1][Ka_2]}$$

$$\delta_{VCR^+} = \frac{[H^+][Ka_1]}{[H^+]^2 + [H^+][Ka_1] + [Ka_1][Ka_2]}$$

$$\delta_{VCR} = \frac{[Ka_1][Ka_2]}{[H^+]^2 + [H^+][Ka_1] + [Ka_1][Ka_2]}$$

Ka_1: Primary equilibrium constant, which represents the equilibrium constant for the ionization of the electrolyte to produce one hydrogen ion and solvent molecule. Ka_2: secondary equilibrium constant, which represents the equilibrium constant for ionization of the electrolyte to produce a second hydrogen ion and solvent molecule.

2.6. The loading kinetics of VCRS liposomes

VCRS liposomes were prepared by loading the drug for 5, 10, 15, 30, 45 and 60 min in a water bath at 35 °C, 45 °C, 55 °C and 65 °C, respectively. The EE% was determined to characterize the kinetics of drug loading and to calculate the activation energy required for the reaction. For a determined ΔpH, the active drug-loading process can be regarded as a one-stage reaction process. The reaction endpoint was the stabilization of the drug concentration in the inner aqueous phase to a constant level.

$$\frac{dC_o}{dt} = -\frac{AP}{V}C_o$$

C_o was the drug content of the external aqueous phase, A was the surface area of the membrane, P was the periplasmic permeability coefficient of the drug, and V was the external aqueous phase volume. A, V and P were fixed constants.

$$\frac{dC_o}{dt} = -\mathrm{k}C_o$$

$$(C_t)_o = (C_0)_o e^{-kt}$$

$$(C_t)_i = \left(C_{eq}\right)_i \left(1 - \mathrm{e}^{-\mathrm{kt}}\right)$$

C_t was the concentration of drug in the internal aqueous phase at moment t, and C_{eq} was the concentration of drug in the internal aqueous phase after equilibrium of drug loading.

$$(E_t)_i = \left(E_{eq}\right)_i \left(1 - e^{-kt}\right)$$

E_t was the EE% at moment t and E_{eq} was the EE% at equilibrium.

The drug loading process in liposomes was closely related to the reaction temperature, and a potential barrier (activation energy Ea) needs to be crossed for VCRS to be encapsulated into the liposomes. The activation energy required for the reaction can be calculated by linear regression of 1/T with lnk according to the Arrhenius formula.

$$k = k_o e^{-Ea/RT}$$

2.7. The degradation of VCRS in release medium

PBS and PBS containing 2.75% butanol (pH 7.4, 6.5 and 5.5) were prepared as different release media, respectively. The release medium was mixed with VCRS solution (100 μg/mL). The mixed solutions were incubated in a water bath shaker at 37 °C. Samples were taken at the designed time points and the concentration was determined by HPLC. The stability of VCRS in the release medium was examined by plotting ln (C/C_0) against time (t).

2.8. In vitro release behavior of VCRS liposomes

The release medium was PBS containing 2.75% butanol at pH 7.4, 6.5 and 5.5, respectively. 0.5 mL of VCRS liposomes were pipetted into a dialysis bag (8–14 k Da), put into an Eppendorf tube containing 10 mL of different release medium, and placed in a 37 °C water bath with constant speed vibration. At 0.5, 2, 4, 6, 8, 12, 24, 48, 72 and 120 h, 0.5 mL of release medium was taken and 0.5 mL of fresh release medium was replenished. HPLC was used to determine the drug concentration. And the release mechanism of the VCRS liposomes was investigated using zero-order, first-order, Higuchi, and Ritger-peppas models, respectively.

2.9. Cytotoxicity assay

Shenyang Pharmaceutical University provided breast cancer cells (4T1). The 4T1 cells were cultured in RPMI 1640 containing 1% streptomycin/penicillin and 10% FBS. 4T1 cells (4×10^3 cells/well) were cultured into 96-well plates for 12 h. 100 μL of samples at different concentrations (VCRS solution and VCRS liposomes) were added and incubated for 24 and 48 h. CCK-8 solution was added and incubation continued for an additional 4 h. Finally, the absorbance was measured at 450 nm using a microplate reader.

2.10. Cellular uptake

Coumarin 6 (C6) was loaded into liposomes to prepare fluorescently labeled liposomes. ESM and cholesterol were weighed precisely, and C6 was weighed precisely under light-avoidance conditions. The drug-lipid ratio was >50:1, and the EE% was close to 100%. The mixture was dissolved in chloroform, and fluorescent liposomes were prepared by thin film hydration-freeze-thaw extrusion method. For C6 solution (C6—S), C6 was dissolved in DMSO and diluted with PBS.

4T1 cells (5×10^4 cells/well) were plated onto coverslips and cultured overnight, and then incubated with C6—S and C6 liposomes (C6-L) (500 ng/mL) for 1 and 3 h, respectively. After incubation, the cells were fixed and stained with DAPI, the intracellular fluorescence was identified under the confocal laser scanning microscope (CLSM, LSM710, ZEISS, Germany). In addition, the intracellular fluorescence intensity values were determined using flow cytometry (BDFACSAria™ III).

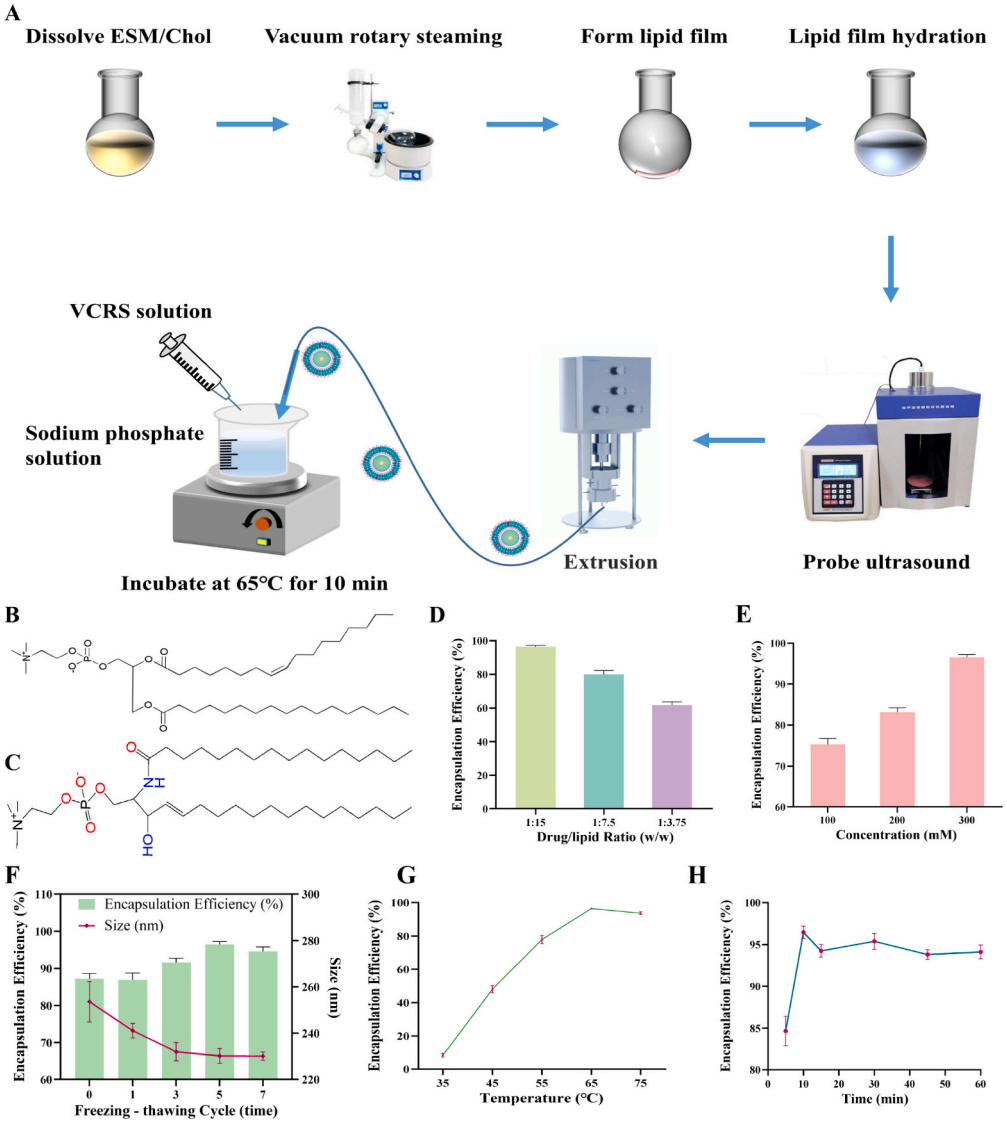

Fig. 1. (A) Schematic diagram of the preparation of VCRS liposomes. The molecular structure of (B) PC and (C) ESM. The effect of (D) drug-to-lipid ratio and (E) concentration of citrate buffer on the encapsulation efficiency of VCRS liposomes ($n = 3$). (F) The effect of freeze-thaw cycle on the particle size and encapsulation efficiency of VCRS liposomes (n = 3). The effect of drug loading (D) temperature and (E) incubation time on the encapsulation efficiency of VCRS liposomes (n = 3).

2.11. Animals

All animal experiments were performed following the National Research Council's Guide for the Care and Use of Laboratory Animals. Shenyang Pharmaceutical University Animal Center provided 6–8 weeks female BALB/c mice (20–25 g). Humane care practices were employed to provide appropriate housing, feeding, and handling of the mice. All animal experiments were performed under the Guidelines for the Ethical Review of Laboratory Animal Welfare, a People's Republic of China National Standard (China, GB/T35892–2018) and the Shenyang Pharmaceutical University's Animal Ethics Committee issued the approval for all experimental procedures involving mice.

2.12. In vivo antitumor effect

4T1 cells (5×10^5 cells/mice) were subcutaneously injected in the right armpit of female BALB/c mice to establish the tumor xenograft model. When the tumor volume was nearly 90 mm^3, the mice were randomly divided into six groups: saline, VCRS solution (1 mg/kg and 1.5 mg/kg), VCRS liposomes (1 mg/kg, 1.5 mg/kg and 2.5 mg/kg) ($n = 5$). All were administered by tail vein injection, once a week for a total of 2 doses. The tumor volume and body weight were monitored every 2 days. Furthermore, the tumor volume was calculated. At the end of experiment, the mice were euthanized on day 14, and the tumors were collected, weighed and photographed.

$$Tumor\ volume\ (mm^3) = \frac{Length \times Width^2}{2}$$

2.13. Toxicity evaluation

On day 14, the serum of mice was collected. The serum levels of Alanine aminotransferase (ALT), Aspartate aminotransferase (AST), Alkaline phosphatase (ALP), Creatinine (CR) and Uric acid (UA) were measured by Chemray 240 automatic biochemical analyzer to check for liver and kidney function. The major organs (heart, liver, kidney, spleen and lung) as well as tumors were removed from the mice after execution on day 14, washed with saline and fixed in 4% paraformaldehyde solution. The tissues were dehydrated, paraffin-embedded, sectioned and then stained with hematoxylin-eosin (H&E). The cytomorphological changes of the tumor and organ tissues were observed under the microscope.

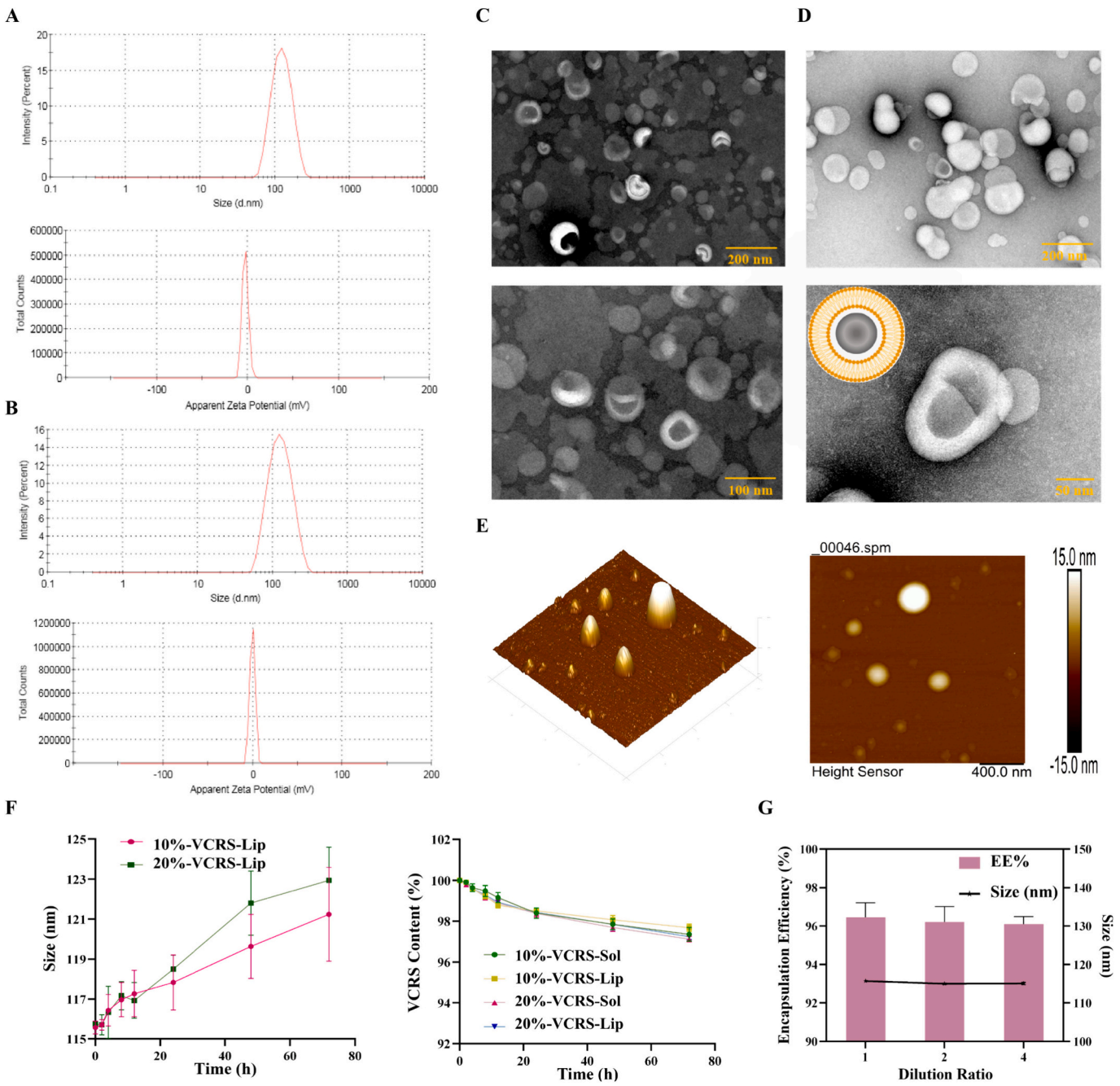

Fig. 2. The particle size and zeta potential of (A) blank liposomes and (B) VCRS liposomes. TEM images of (C) blank liposomes and (D) VCRS liposomes. (E) AFM images of VCRS liposomes. (F) The stability of VCRS liposomes in plasma (n = 3). (G) The dilution stability of VCRS liposomes (n = 3).

2.14. Statistical analysis

Data were represented as mean ± SD. Data were performed using the one-way ANOVA test. Statistical differences were considered significant when the p value was lower than 0.05.

3. Results and discussion

3.1. Preparation of VCRS liposomes

VCRS is an amphiphilic drug, which is suitable for the preparation of liposomes by the active loading method to obtain a high encapsulation efficiency. The pH gradient method is suitable for the transmembrane gradient loading of weakly alkaline drugs. The extra-membrane pH induces the drug to exist in the form of molecules which is favorable for the crossing of the lipid membrane. And the intra-membrane pH induces the drug to change into the form of ions, which reduces the permeability and completes the drug encapsulation. Therefore, it is proposed to use pH gradient method for active drug loading of VCRS, and the process route mainly includes the preparation of blank liposomes and drug-loaded liposomes (Fig. 1A). The blank liposomes were prepared by thin film hydration-freeze-thaw extrusion method. The pH gradient of blank liposomes was not established by the conventional method (external aqueous phase substitution), but the innovative addition of pH-adjusting solution. The drug-loading process involved mixing and incubating the drug solution, blank liposomes with the pH-adjusting solution. The prescription and process were also examined to determine the optimal prescription and process route for VCRS liposomes.

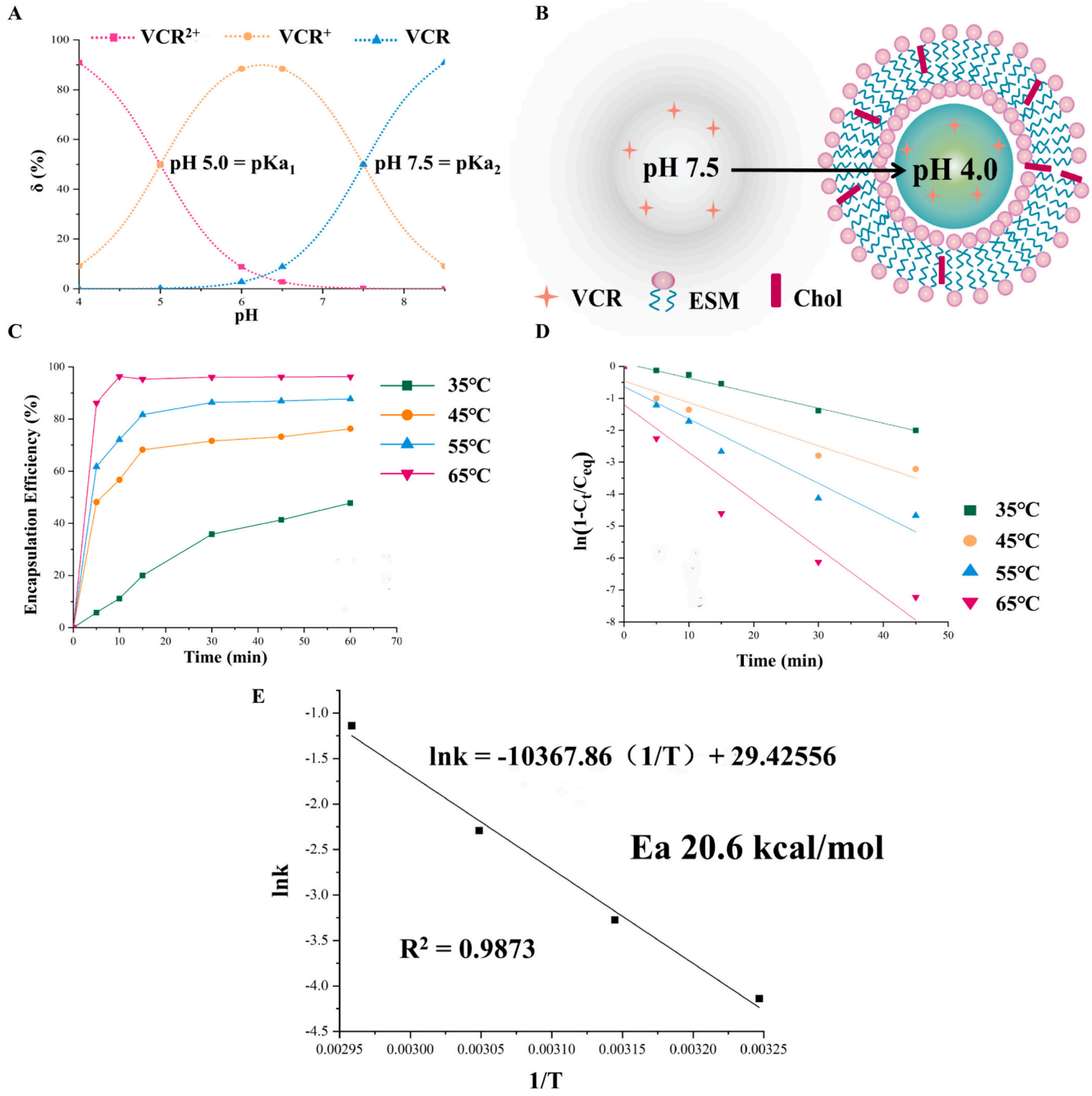

Fig. 3. (A) The δ% of VCR with pH. (B) The schematic diagram of the pH gradient method for active drug loading. (C) The encapsulation efficiency curve with time at different temperatures. (D) The curve of linear regression equation for $\ln(1-C_t/C_{eq})$. (E) The Ea of liposomes on drug loading process.

Phospholipids, as the main membrane material of liposomes, affect the particle size, encapsulation efficiency, stability, and *in vivo* distribution of liposomes. As Table S1 illustrated, liposomes prepared from the three phospholipids and cholesterol (2.5:1, w) showed little difference in particle size and PDI, but the ESM liposomes exhibited a higher EE%. Both E80 and S100 are mixed phospholipids whose main component is phosphatidylcholine (PC), which is structurally a glycerophospholipid (Fig. 1B). Sphingomyelin (SM) is a typical sphingomyelin phospholipid with two hydrophobic tail chains, sphingomyelin and amide (Fig. 1C)(Slotte, 2016). Compared to PC, SM is capable of forming inter- and intramolecular hydrogen bonds, and it can form a stable hydrogen bonding network that interacts more closely with cholesterol. These structural features make the hydrophobic region of SM molecules more saturated, with better symmetry, and more tightly bound to cholesterol after forming lipid bilayers(McIntosh et al., 1992; Samsonov et al., 2001). Therefore, ESM has a higher phase transition temperature and a more stable structure(Hwang et al., 1980), while S100 and E80 have a low phase transition temperature, which cannot form a dense structure. Moreover, the hydrolysis tolerance of amide bond is better than that of ester bond, so ESM with good stability and high EE% was chosen as the membrane material. As Fig. 1D shown, the EE% gradually decreased with the increase of the drug/lipid ratio. The highest EE% was achieved at 1:15 (w). Positively charged VCRS exists mostly in molecular form in the neutral or weakly alkaline environment of the outer aqueous phase. After passing through the lipid bilayer, it combines with the H^+ of the inner aqueous phase and transforms into ionic form. The

more VCRS, the more H^+ is consumed, the drug can't continue to enter the inner aqueous phase, and the EE% is reduced.

The higher the concentration of buffer in the hydration medium, the more H^+ was present, contributing to an increase in the VCRS bound to H^+ and an increase in the EE% (Fig. 1E). The ability of liposomes to load VCRS was directly related to the ΔpH inside and outside the membrane. The salt concentration was too low, resulting in incomplete hydration of the liposomes. In summary, 300 mM citrate buffer with the highest EE% was chosen as the hydration medium. The presence of salts led to a swelling of the lamellar phase mainly driven by the weakening of the van der Waals attraction (Chemin et al., 2008). With the increase of the number of freeze-thaw cycles, the EE% gradually increased and the particle size gradually decreased (Fig. 1F). Through the freeze-thaw cycle process, the lipid bilayer is damaged by solid ice and the lipid membrane is fractured or partially broken. Due to the hydrophobic effect, the damaged lipid membrane will be reassembled, and multilayer liposomes can be transitioned to monolayer liposomes. The use of freeze-thaw cycles can balance the concentration of the internal aqueous phase of liposomes, improve lipid accumulation, and increase the encapsulation efficiency(Costa et al., 2014). The encapsulation efficiency decreased after the freeze-thaw cycle was carried out for seven times, mainly because repeated freeze-thaw destroys the integrity of liposomes. Therefore, the freeze-thaw cycle process was selected to be performed 5 times.

The EE% of liposomes increased gradually with increasing the drug loading temperature. The drug loading temperature of liposomes is closely related to the phase transition temperature of phospholipids. When the temperature is higher than the phase transition temperature, the phospholipid fatty chain is transformed from a compact all-trans conformation (gelatinous crystalline state) to a lax neighbor-crossing form (liquid crystal state), which substantially increases the radius of rotation. At the same time the form of hydrogen bonding changes from intermolecular to intramolecular hydrogen bonding(Slotte, 2016). The structural change of the phospholipid molecules induces an increase in their active space, which in turn enhances the mobility and permeability of the liposomes and facilitates the loading of the drug into the internal aqueous phase. The highest EE% was achieved at a temperature of 65 °C (Fig. 1G). Continuing to increase the temperature, on the one hand, it will prompt the outflow of the buffer of the inner aqueous phase, reduce the driving force of drug loading, and lower the EE%. On the other hand, it will accelerate the oxidation of phospholipids and destabilize the liposomes. For incubation time, the EE% could reach about 85% at 5 min, and reached the maximum at 10 min, and then stabilized (Fig. 1H). In view of the fact that prolonged high-temperature loading will increase the oxidation of phospholipids and the degradation of the drug, 10 min was chosen as the incubation time for drug loading.

Thus, ESM and cholesterol (2.5:1, w) were dissolved in chloroform, the drug/lipid ratio was 1:15 (w). Chloroform was evaporated while lipid films were prepared. Citrate solution (300 mM) was used as the hydration medium. The obtained large particle size liposomes were subjected to probe sonication, freeze-thaw cycles (−80 °C ~ 65 °C, 5 times) and were extruded at 65 °C. Blank liposomes and drug solutions (1 mg/mL) were placed in the external aqueous solution (1:5:25, v), magnetically stirred, and incubated in a water bath at 65 °C for 10 min. Then VCRS liposomes were prepared and stored at 4 °C. Compared to the patent of Marqibo®, we described the process of VCRS liposomes in details, which can be able to easily produce.

3.2. Characterization of VCRS liposomes

Blank liposomes were milky white liquids and VCRS liposomes were translucent milky blue liquids (Fig.S3). The particle size of blank liposomes and VCRS liposomes were about 110 nm, the zeta potential was close to 0 mV, mainly due to ESM being a neutral phospholipid with no charge (Fig. 2A, B). Blank liposomes were spherical with uniform size and rounded particles under TEM (Fig. 2C). VCRS liposomes were irregular spheres, which might be related to the presence state of the drug within the liposomes (Fig. 2D). VCRS liposomes observed by AFM were spherical particles with smooth and flat surface and no agglomerates (Fig. 2E). The content of ESM and VCRS were close to 100%, and the EE% were above 95%. As Table S2 illustrated, after being placed at room temperature for 3 months, the particle size of VCRS liposomes slightly increased, and the EE% and content decreased to some extent, but the changes were small, indicating a certain degree of stability. The results of long-term test showed that the liposomes had good stability after being placed under low temperature for 6 months (Table S3). As shown in Fig. 2F, the particle size of 10% and 20% liposomes in plasma increased slightly within 72 h, indicating that VCRS liposomes could exist more stably in plasma. After encapsulating VCRS into liposomes, the difference in drug content between the liposomes group and the solution group was relatively small, indicating that the plasma stability of the drug itself was not affected by the carrier. Normally, liposomes are diluted with saline for intravenous administration. The physicochemical properties of VCRS liposomes were not affected after dilution (Fig. 2G). The good results of stability in use provided a guarantee for intravenous administration.

3.3. The loading kinetics of VCRS liposomes

The core of pH gradient method for active drug loading is to establish ΔpH inside and outside the membrane(Qiu et al., 2008). VCR is molecular form in the extra-membrane medium and easily passes through the membrane. After entering the aqueous phase, under acidic conditions, it transforms into ionic drug, and the ionic VCR is not easy to penetrate the lipid bilayer membrane, and the encapsulation of the drug is completed through this process. Therefore, calculating the relationship between δ% and pH for each form of VCR is a necessary prerequisite for the establishment of ΔpH. At pH = 4.0, $[VCR^{2+}]$ was 9 times that of $[VCR^+]$, and [VCR] was almost absent in aqueous solution, so it could be taken as the pH of the inner aqueous phase of the liposomes (Fig. 3A). According to the Henderson - Hasselbalch theory(Hills, 1973), for every change of 1 pH unit, a 10-fold difference in the concentration of the molecular *versus* ionic drug is generated. To ensure a high EE%, it was theoretically necessary to produce a 1000-fold difference in concentration, *i.e.*, a pH gradient of 3 pH units. Under the condition of determining the pH of the inner aqueous phase = 4, the pH of the outer aqueous phase should be 7. However, the VCR was a dibasic base, and at this time, [VCR] was smaller than $[VCR^+]$, and the proportion of ionic drug was larger, which was unfavorable for the drug to enter into the liposomes through the membrane. And when pH = 7.5, [VCR] was equal to $[VCR^+]$, at this time, the molecular-type drug accounts for a higher proportion, which can be encapsulated through the lipid bilayer. The ionic drug in the outer aqueous phase was prompted to shift to the molecular type, and the ionization equilibrium was shifted to the left, thus completing the encapsulation of all drugs. The ΔpH inside and outside the membrane was thus established to be 3.5 pH units, *i.e.*, pH = 4.0 for the inner aqueous phase and pH = 7.5 for the outer aqueous phase (Fig. 3B).

As Fig. 3C shown, the EE% increased with increasing temperature for the same incubation time, which was mainly related to the phase transition temperature of liposomes. On the other hand, the reaction time required for the EE% to reach equilibrium was negatively correlated with temperature. The Arrhenius formula stated that temperature could increase the reaction rate, which was consistent with the results. Fig. 3D showed the first-order fit of the EE% to the time curve at each temperature. The results showed good linearity in each group, and the fitted curves at 35 °C, 45 °C, 55 °C and 65 °C showed correlation coefficients of 0.9942, 0.9683, 0.9426 and 0.9345, respectively, which proved that the process of VCRS capture by liposomes conformed to the first-order kinetic model. Fig. 3E showed that lnk had a good linear phase system for 1/T, and k was positively correlated with the reaction temperature. When the influencing factors such as the composition of liposomes, drug

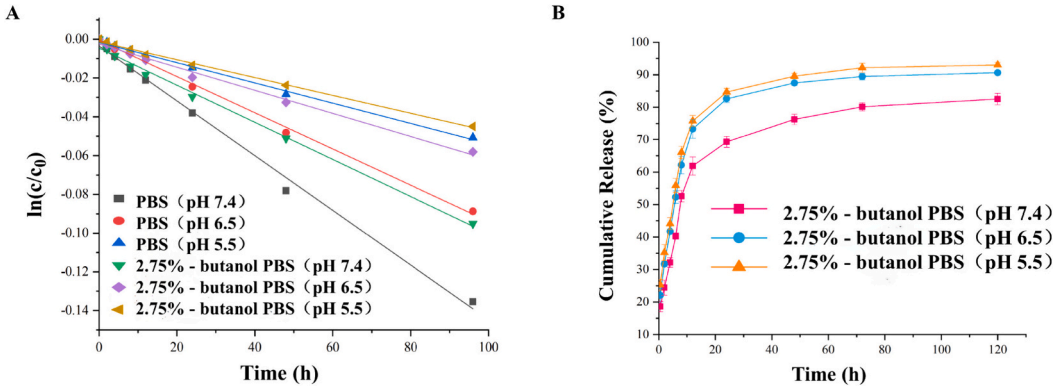

Fig. 4. (A) The stability of VCRS in PBS (pH 7.4, 6.5 and 5.5) and PBS containing 2.75%- butanol (pH 7.4, 6.5, and 5.5). (B) The release curve of VCRS liposomes in PBS containing 2.75%- butanol (pH 7.4, 6.5 and 5.5) ($n = 3$).

Table 1
Modeling equation for the release of VCRS liposomes in PBS containing 2.75%-butanol.

	pH 7.4	pH 6.5	pH 5.5
Zero-order	$Q = 0.51\ t + 37.98$ ($R^2 = 0.6634$)	$Q = 0.45\ t + 44.20$ ($R^2 = 0.7294$)	$Q = 0.32\ t + 61.38$ ($R^2 = 0.4369$)
First-order	**$Q = 78.42(1\text{-}e^{-0.13t})$ ($R^2 = 0.9393$)**	**$Q = 89.01(1\text{-}e^{-0.98t})$ ($R^2 = 0.9831$)**	**$Q = 90.63(1\text{-}e^{-0.17t})$ ($R^2 = 0.9267$)**
Higuchi	$Q = 6.56\ t^{1/2} + 24.13$ ($R^2 = 0.8541$)	$Q = 6.00\ t^{1/2} + 31.72$ ($R^2 = 0.8654$)	$Q = 4.96\ t^{1/2} + 46.19$ ($R^2 = 0.6704$)
Ritger-peppas	$Q = 26.34\ t^{0.26}$ ($R^2 = 0.9298$)	$Q = 31.75\ t^{0.23}$ ($R^2 = 0.9280$)	$Q = 42.27\ t^{0.17}$ ($R^2 = 0.8525$)

model and loading gradient were determined, the activation energy required for the reaction was a constant value. The activation energy for the drug-loading reaction was calculated to be 20.6 kcal/mol. The drug-loading gradient of pH = 4 in the inner aqueous phase and pH = 7.5 in the outer aqueous phase (ΔpH was 3.5 pH units) was established. The drug-loading process of liposomes showed first-order kinetic, the drug-loading rate gradually decreased with time, and the time for the drug-loading to reach equilibrium was shortened with the increase of temperature. The activation energy of the liposome drug-loading reaction was 20.6 kcal/mol.

3.4. The release kinetics of VCRS liposomes

The main degradation route for VCRS in an aqueous environment is hydrolysis(Wenxue et al., 2019). The degradation of VCRS in PBS

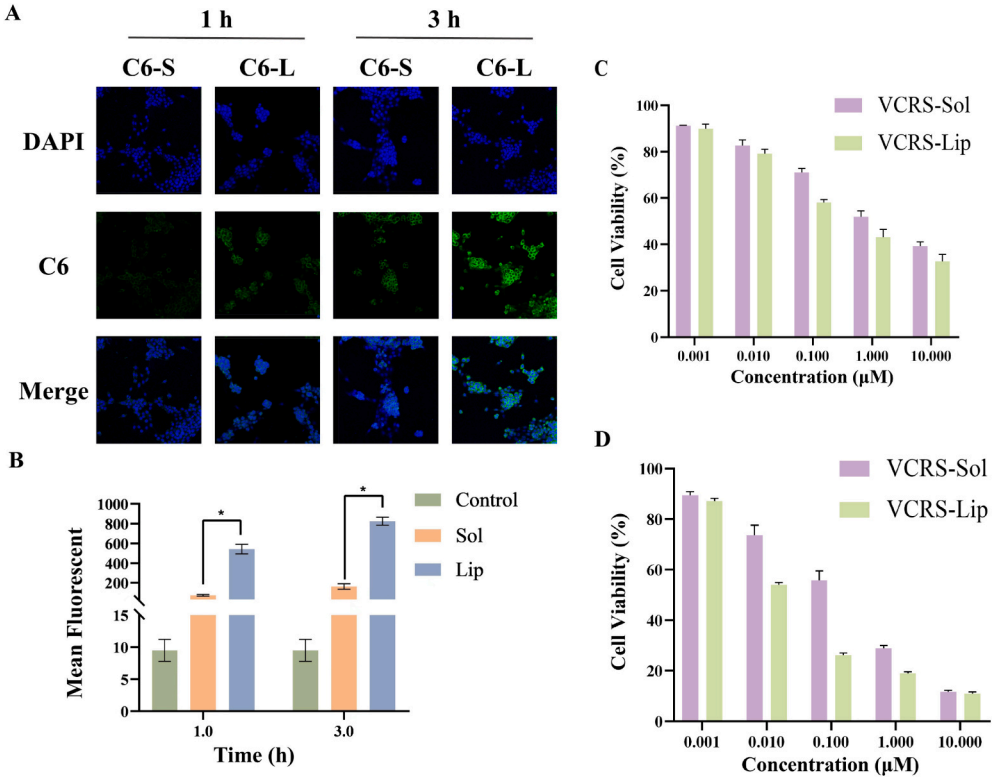

Fig. 5. (A) CLSM images of 4T1 cells after incubation with C6 solution and C6 liposomes for 1 h and 3 h (×200). (B) Intracellular fluorescence of 4T1 cells after incubation with C6 solution and C6 liposomes for 1 h and 3 h recorded by a flow cytometry ($n = 3$) (*$P < 0.05$).4T1 cells viability after treatment with different concentrations of VCRS solution and VCRS liposomes for (C) 24 h and (D) 48 h ($n = 5$).

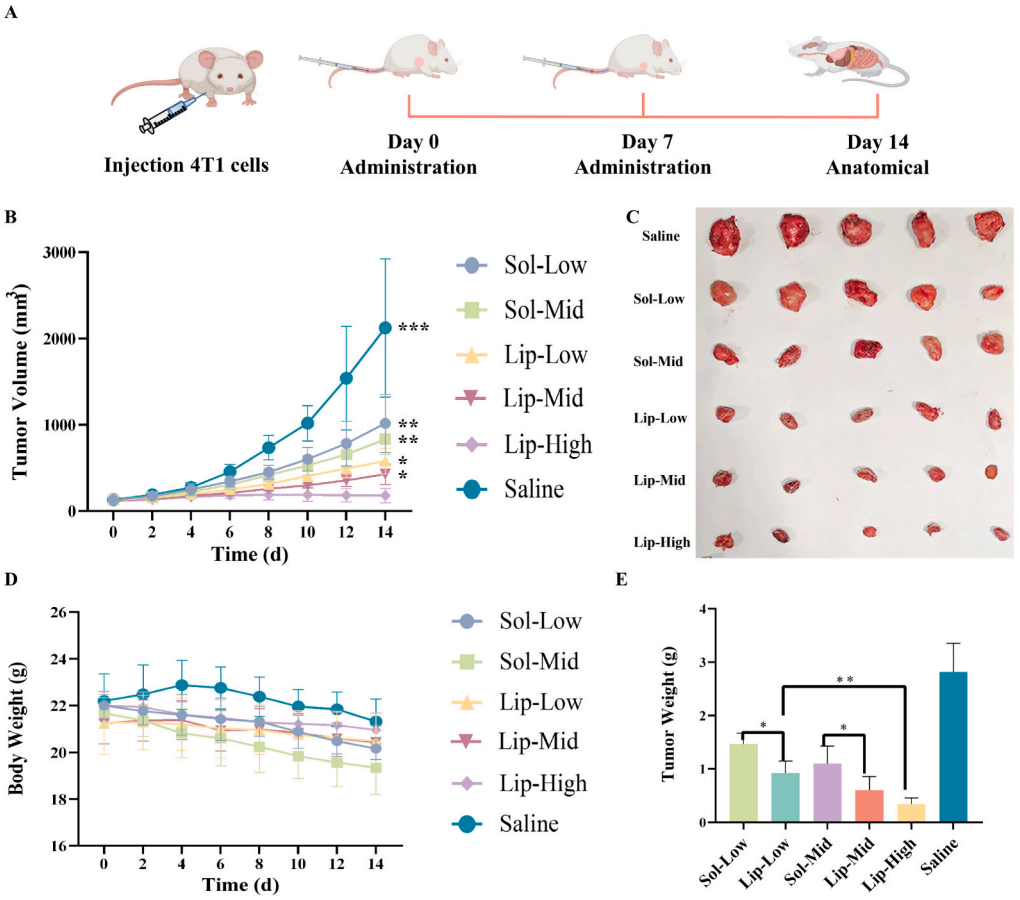

Fig. 6. (A) Schematic diagram of pharmacodynamics research. (B) The tumor volume of mice after intravenous administration ($n = 5$). * *VS* Lip-High, ***$P < 0.001$, **$P < 0.01$, *$P < 0.05$. (C) Photograph of tumors (n = 5). (D) The body weight of mice after intravenous administration (n = 5). (E) Tumor weight of the respective group at the end of experiment (n = 5). **P < 0.01, *P < 0.05.

conformed to a first-order kinetic model (Fig. 4A). The degradation rate of VCRS increased with increasing pH, which was attributed to the fact that weakly basic drugs were usually more stable in acidic environments. The degradation of VCRS was slower in PBS containing 2.75% butanol than in PBS, indicating that a certain concentration of butanol inhibits the degradation of the drug in PBS. The release of VCRS liposomes were close to 20% within 0.5 h, and the release of VCRS liposomes were about 70% at 24 h, with a more complete release at 120 h and the cumulative release of >90% (Fig. 4B). As Fig. 4B shown, the cumulative release and release rate of VCRS at pH 6.5 and 5.5 were higher than that at pH 7.4. Due to the pH of the release medium was 6.5 and 5.5, and the pH of the aqueous phase in the liposomes was 7.5. The pH was characterized by an internal high and an external low in liposomes, promoting the release of the drug from the internal aqueous phase into the medium. The VCRS liposomes showed the trend of faster and more complete release under the low pH condition. This suggested that VCRS liposomes could function in the tumor environment.

The results of release kinetic equation fitting showed that the release behavior of VCRS liposomes was more in line with the first-order model (correlation coefficients of 0.9393, 0.9831 and 0.9267 for pH 7.4, 6.5 and 5.5, respectively) and Ritger-peppas (correlation coefficients of 0.9298, 0.9280 and 0.8525 for pH 7.4, 6.5 and 5.5, respectively) (Table 1). A closer fit with the first-order model suggested that the drug was released from liposomes by simple transmembrane diffusion. The release mechanism may be related to the way of VCRS was present in the liposomes. The release indices for pH 7.4, 6.5 and 5.5 in the Ritger-peppas model were 0.26, 0.23 and 0.17, respectively, which were <0.45, suggesting that the mechanism of release of the drug was simple transmembrane diffusion(Liu et al., 2021a). These showed that the *in vitro* release of VCRS liposomes conformed to a first-order kinetic process with a fast and then slow-release rate. The release mechanism of VCRS liposomes was simple transmembrane diffusion. It also showed a tendency for faster and more complete release under low pH conditions in tumors, which was conducive to effective drug delivery.

3.5. *In vitro anti-tumor effect*

The intensity of intracellular green fluorescence (C6) at 3 h was significantly higher than that at 1 h, and the cellular uptake showed time-dependence. At the same time, the intracellular fluorescence intensity was significantly stronger in the C6 liposomes group than in the C6 solution group (Fig. 5A). This indicated that liposomes were more readily taken up by cells compared to free solutions. The intensity of intracellular fluorescence gradually increased with the prolong of incubation time. Meanwhile, the intracellular fluorescence intensity in the liposomes group was significantly higher than that in the solution group (Fig. 5B). The composition and structure of liposomes are similar to that of cell membranes, so they have better cell affinity and can enhance the uptake of liposomes by cells. The interaction between liposomes and cells can be categorized into four mechanisms: adsorption, lipid exchange, endocytosis and fusion(Liu et al., 2022). Among them, endocytosis is the main mechanism of liposome-cell interaction. Therefore, encapsulating VCRS within liposomes can effectively enhance cellular uptake.

The results of cytotoxicity were shown in Fig. 5C, D, the cell viability of both solution and liposomes gradually decreased with the increase of time and concentration, showing the time-dependent and concentration-dependent inhibition of tumor cell growth by VCRS. The cell viability of

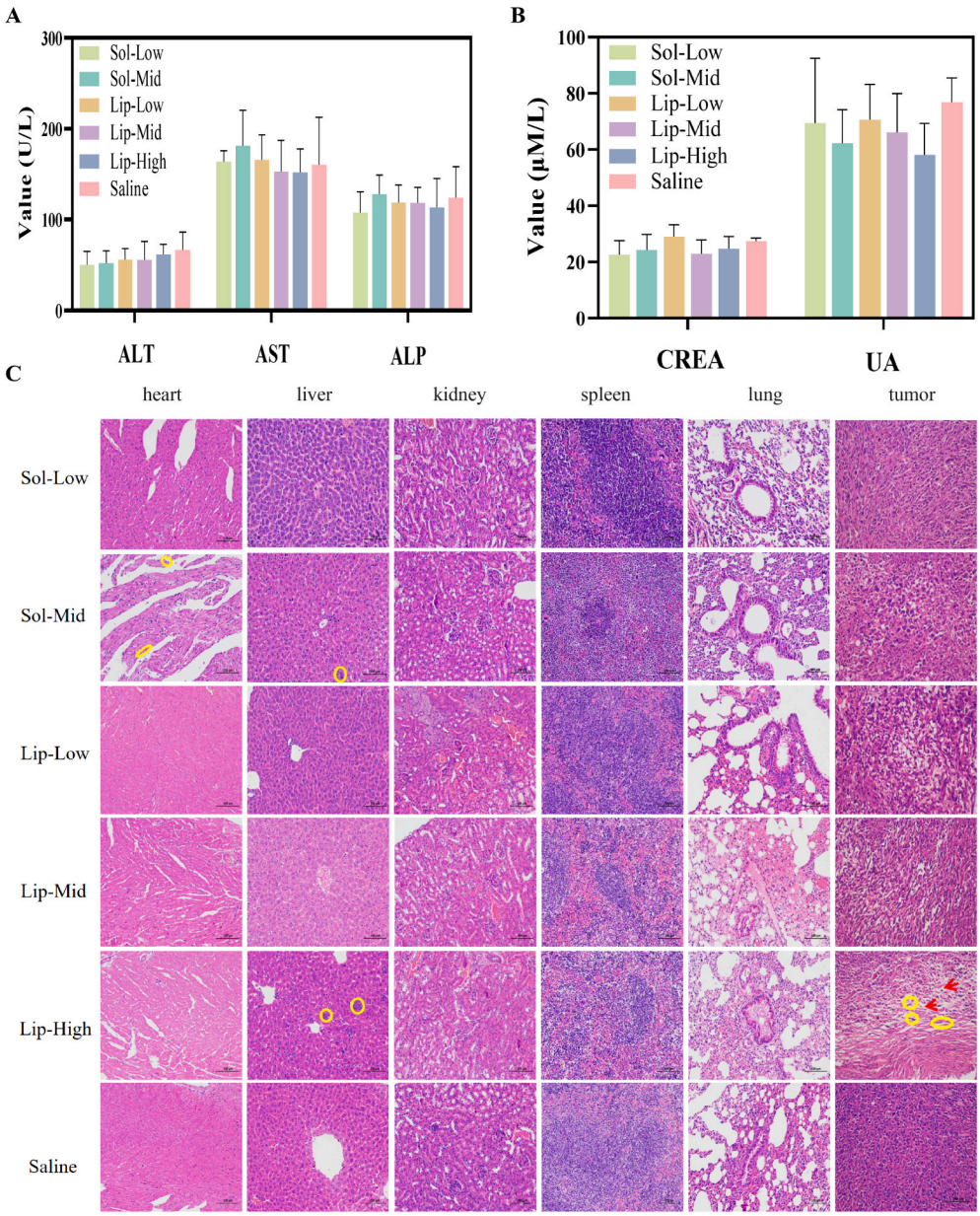

Fig. 7. The serum levels of markers for (A) liver function and (B) kidney function (n = 5). (C) H&E staining images of the major organs and tumors (n = 3) (×200).

liposomes was lower than that of free solution. The IC_{50} of VCRS solution and VCRS liposomes for 4T1 cells at 24 h was 0.326 and 0.081 μM, respectively. The IC_{50} of VCRS solution and VCRS liposomes at 48 h was 0.139 and 0.034 μM, respectively. These indicated that VCRS liposomes had an improved cytotoxic effect. VCR is a highly active cell cycle-dependent anticancer drug. It binds to tubulin causing microtubule depolymerization, metaphase arrest and apoptotic death of cells undergoing mitosis(Gidding et al., 1999). Tubulin is essential for the normal polymerization of mitotic spindle microtubules. VCR binding to spindle microtubules alters spindle structure and function in a concentration-dependent manner. Interference of microtubule function also disrupts other cellular processes that involve microtubules, such as intracellular transport and cellular organization(Degraeve, 1978). As a result of its interruption of microtubule function, especially evident during M-phase, cells accumulate in metaphase contributing to VCR-induced cytotoxicity(Suter et al., 1980). VCRS liposomes inhibited cell growth more than free solution, which may be due to the stronger uptake of liposomes than solution. SM is one of the components of the extracellular membrane, which is biocompatible with the cell membrane, and has a better affinity performance for the cell membrane. Liposomes can be more readily taken up by cells through membrane fusion compared to solution, then inhibited proliferation.

3.6. *In vivo anti-tumor effect*

To evaluate antitumor effects *in vivo*, 4T1 tumor-bearing BALB/C mice were selected and intravenously administered with VCRS solution and VCRS liposomes (Fig. 6A). The 4T1 tumor-bearing mice were randomly divided into six groups, namely, the low-dose VCRS solution group (Sol-Low, 1 mg/kg), the medium-dose solution group (Sol-Mid, 1.5 mg/kg), the low-dose VCRS liposomes group (Lip-Low, 1 mg/kg), the medium-dose liposomes group (Lip-Mid, 1.5 mg/kg), the high-dose liposomes group (Lip-High, 2.5 mg/kg) and the saline group (n = 5). According to Fig. 6B, compared to the saline group, all administration groups significantly decreased the tumor volume ($p < 0.05$). The tumor volume on day 14, saline> Sol-Low> Sol-Mid > Lip-Low> Lip-Mid > Lip-High. Among all groups, the Lip-High group presented the lowest tumor volume. The tumor volume of the Lip-High group showed

minimal change, and there was a difference between the Lip-High group and other groups ($p < 0.05$). As Fig. 6C, E delineated, at equivalent doses, the VCRS liposome groups manifested superior antitumor activity when contrasted with the VCRS solution groups ($p < 0.05$). The tumor weight of the Lip-High group was 0.12-fold than that in the saline group, 0.23-fold than that in the Sol-Low group, 0.31-fold than that in the Sol-Mid group, 0.37-fold than that in the Lip-Low group, 0.57-fold than that in the Lip-Mid group. Thus, the Lip-High group demonstrated the most efficacious antitumor activity. These confirmed that VCRS liposomes could achieve an enhanced antitumor effect *in vivo*.

There was no significant difference between the saline group and other groups in body weight ($p > 0.05$), but the body weight of the solution groups was slightly decreased (Fig. 6D). And the body weight of the VCRS liposomes groups (even at high dose) wasn't decreased. The values of the relevant indexes of liver and kidney function in each dosing group were within the reference range, and there was no significant difference compared with the control group ($p > 0.05$) (Fig. 7A, B). None of the dosing groups caused serious damage to the liver and kidney functions of the mice. In liver tissue sections, a small number of blue parenchymal cell aggregates (yellow circles) were observed (Fig. 7C). Presumably, immune cells in the liver were phagocytizing other substances and an inflammatory response was suspected to be occurring. Broken nuclei and disorganized morphology were observed in the myocardial tissue of the solution group, suggesting that the cardiomyocytes were slightly damaged (Fig. 7C). In the tumor tissue sections, the cancer cells in the saline group were growing vigorously and were in a period of rapid proliferation. However, the nuclei of tumor cells in the rest of the administered groups showed solidification, deformation, fragmentation and incompleteness. It indicated that the tumors in all groups had different degrees of tissue necrosis. The blank areas (red arrows) were presumed to be left by the lysis of necrotic tissues after the killing of tumor cells by VCRS, with the Lip-High group having the largest number of empty cavities, indicating the best antitumor activity (Fig. 7C). These suggested that VCRS liposomes had a stronger antitumor effect compared to VCRS solution and had a favorable biosafety profile.

4. Conclusions

In this article, we proposed to use the pH gradient method for active drug loading of VCRS, and the process route mainly included the preparation of blank liposomes and drug-loaded liposomes. The blank liposomes were prepared by thin film hydration-freeze-thaw extrusion method. The drug-loading process involved mixing and incubating the drug solution, blank liposomes with the pH-adjusting solution. VCRS liposomes had suitable particle size, high encapsulation efficiency and good stability. The drug-loading process of liposomes exhibited a first-order kinetic feature, and the activation energy required for the reaction was determined as 20.6 kcal/mol. The release behavior conformed to the first-order model, suggesting that the release mechanism of VCRS was transmembrane diffusion. VCRS liposomes also enhanced *in vitro* and *in vivo* antitumor activity. Thus, VCRS liposomes showed great potential for VCRS delivery, and the loading and release kinetics were well researched to play foundation for better explore liposomes.

CRediT authorship contribution statement

Zixu Liu: Writing – original draft, Visualization, Formal analysis, Data curation, Conceptualization. **Yang Liu:** Writing – original draft, Visualization, Formal analysis, Data curation, Conceptualization. **Zixuan Wu:** Visualization, Software, Methodology, Formal analysis. **Boyuan Liu:** Visualization, Methodology, Formal analysis. **Linxuan Zhao:** Writing – original draft, Visualization. **Tian Yin:** Methodology, Investigation. **Yu Zhang:** Validation, Data curation. **Haibing He:** Supervision, Investigation. **Jingxin Gou:** Methodology, Investigation. **Xing Tang:** Writing – review & editing, Writing – original draft, Supervision, Investigation, Funding acquisition, Conceptualization. **Song Gao:** Writing – review & editing, Writing – original draft, Supervision, Funding acquisition, Conceptualization.

Declaration of competing interest

The authors declare no competing financial interest.

Data availability

Data will be made available on request.

Acknowledgment

This work was supported by Liaoning Livelihood Science and Technology Plan Joint Project (No. 2023JH2/101700135), National Key Research and Development Program of China (No.2020YFE0201700), and 345 Talent Project, Shengjing Hospital of China Medical University (No.M1419).

Appendix A. Supplementary data

Supplementary data to this article can be found online at https://doi.org/10.1016/j.ijpx.2024.100258.

References

Bangham, A.D., Standish, M.M., Watkins, J.C., 1965. Diffusion of univalent ions across the lamellae of swollen phospholipids. J. Mol. Biol. 13, 238–IN227.
Becker, S., Kiecke, C., Schäfer, E., Sinzig, U., Deuper, L., Trigo-Mourino, P., Griesinger, C., Koch, R., Rydzynska, Z., Chapuy, B., von Bonin, F., Kube, D., Venkataramani, V., Bohnenberger, H., Leha, A., Flach, J., Dierks, S., Bastians, H., Maruschak, B., Bojarczuk, K., Taveira, M., Trümper, L., Wulf, G., Wulf, G., 2020. Destruction of a Microtubule-Bound MYC Reservoir during Mitosis Contributes to Vincristine's Anticancer activity. Mol. Cancer Res. : MCR 18, 859–872.
Chemin, C., Bourgaux, C., Péan, J.-M., Pabst, G., Wüthrich, P., Couvreur, P., Ollivon, M., 2008. Consequences of ions and pH on the supramolecular organization of sphingomyelin and sphingomyelin/cholesterol bilayers. Chem. Phys. Lipids 153, 119–129.
Chen, J., Li, S., Shen, Q., He, H., Zhang, Y., 2011. Enhanced cellular uptake of folic acid–conjugated PLGA–PEG nanoparticles loaded with vincristine sulfate in human breast cancer. Drug Dev. Ind. Pharm. 37, 1339–1346.
Costa, A.P., Xu, X., Burgess, D.J., 2014. Freeze-Anneal-Thaw Cycling of Unilamellar Liposomes: effect on Encapsulation Efficiency. Pharm. Res. 31, 97–103.
Davis, T., Farag, S., 2013. Treating relapsed or refractory Philadelphia chromosome-negative acute lymphoblastic leukemia: liposome-encapsulated vincristine. Int. J. Nanomedicine 8, 3479–3488.
Degraeve, N., 1978. Genetic and related effects of Vinca rosea alkaloids. Mutat. Res./Rev. Genet. Toxicol. 55, 31–42.
Douer, D., 2016. Efficacy and Safety of Vincristine Sulfate Liposome Injection in the Treatment of Adult Acute Lymphocytic Leukemia. Oncologist 21, 840–847.
Fujimura, T., Kakizaki, A., Kambayashi, Y., Sato, Y., Tanita, K., Lyu, C., Furudate, S., Aiba, S., 2018. Cytotoxic antimelanoma drugs suppress the activation of M2 macrophages. Exp. Dermatol. 27, 64–70.
Gidding, C.E.M., Kellie, S.J., Kamps, W.A., de Graaf, S.S.N., 1999. Vincristine revisited. Crit. Rev. Oncol. Hematol. 29, 267–287.
Hagemeister, F., Rodriguez, M.A., Deitcher, S.R., Younes, A., Fayad, L., Goy, A., Dang, N. H., Forman, A., McLaughlin, P., Medeiros, L.J., Pro, B., Romaguera, J., Samaniego, F., Silverman, J.A., Sarris, A., Cabanillas, F., 2013. Long term results of a phase 2 study of vincristine sulfate liposome injection (Marqibo®) substituted for non-liposomal vincristine in cyclophosphamide, doxorubicin, vincristine, prednisone with or without rituximab for patients with untreated aggressive non-Hodgkin lymphomas. Br. J. Haematol. 162, 631–638.
Harding, S.M., Benci, J.L., Irianto, J., Discher, D.E., Minn, A.J., Greenberg, R.A., 2017. Mitotic progression following DNA damage enables pattern recognition within micronuclei. Nature 548, 466–470.
Harmon, B.V., Takano, Y.S., Winterford, C.M., Potten, C.S., 1992. Cell death induced by vincristine in the intestinal crypts of mice and in a human Burkitt's lymphoma cell line. Cell Prolif. 25, 523–536.
Hills, A.G., 1973. pH and the Henderson-Hasselbalch equation. Am. J. Med. 55, 131–133.
Huwyler, J., Drewe, J., Krähenbühl, S., 2008. Tumor targeting using liposomal antineoplastic drugs. Int. J. Nanomedicine 3, 21–29.
Hwang, K.J., Luk, K.F., Beaumier, P.L., 1980. Hepatic uptake and degradation of unilamellar sphingomyelin/cholesterol liposomes: a kinetic study. Proc. Natl. Acad. Sci. 77, 4030–4034.
Johnston, M.J.W., Semple, S.C., Klimuk, S.K., Edwards, K., Eisenhardt, M.L., Leng, E.C., Karlsson, G., Yanko, D., Cullis, P.R., 2006. Therapeutically optimized rates of drug

release can be achieved by varying the drug-to-lipid ratio in liposomal vincristine formulations. Biochim. Biophys. Acta Biomembr. 1758, 55–64.
Jordan, M., Himes, R., Wilson, L., 1985. Comparison of the effects of vinblastine, vincristine, vindesine, and vinepidine on microtubule dynamics and cell proliferation in vitro. Cancer Res. 45, 2741–2747.
Kavcic, M., Koritnik, B., Krzan, M., Velikonja, O., Prelog, T., Stefanovic, M., Debeljak, M., Jazbec, J., 2017. Electrophysiological Studies to Detect Peripheral Neuropathy in Children Treated with Vincristine. J. Pediatr. Hematol. Oncol. 39, 266–271.
Li, G.-Z., Hu, Y.-H., Li, D.-Y., Zhang, Y., Guo, H.-L., Li, Y.-M., Chen, F., Xu, J., 2020. Vincristine-induced peripheral neuropathy: a mini-review. NeuroToxicology 81, 161–171.
Liu, Z., Bu, R., Zhao, L., Liu, L., Dong, N., Zhang, Y., Yin, T., He, H., Gou, J., Tang, X., 2021a. Hydrogel-containing PLGA microspheres of palonosetron hydrochloride for achieving dual-depot sustained release. J. Drug Deliv. Sci. Technol. 65, 102775.
Liu, Z., Chu, W., Sun, Q., Zhao, L., Tan, X., Zhang, Y., Yin, T., He, H., Gou, J., Tang, X., 2021b. Micelle-contained and PEGylated hybrid liposomes of combined gemcitabine and cisplatin delivery for enhancing antitumor activity. Int. J. Pharm. 602, 120619.
Liu, H., Kong, Y., Liu, Z., Guo, X., Yang, B., Yin, T., He, H., Gou, J., Zhang, Y., Tang, X., 2022. Sphingomyelin-based PEGylation Cu (DDC)2 liposomes prepared via the dual function of Cu2+ for cancer therapy: Facilitating DDC loading and exerting synergistic antitumor effects. Int. J. Pharm. 621, 121788.
McIntosh, T.J., Simon, S.A., Needham, D., Huang, C.H., 1992. Structure and cohesive properties of sphingomyelin/cholesterol bilayers. Biochemistry 31, 2012–2020.
Mojarad-Jabali, S., Farshbaf, M., Hemmati, S., Sarfraz, M., Motasadizadeh, H., Shahbazi Mojarrad, J., Atyabi, F., Zakeri-Milani, P., Valizadeh, H., 2022. Comparison of three synthetic transferrin mimetic small peptides to promote the blood–brain barrier penetration of vincristine liposomes for improved glioma targeted therapy. Int. J. Pharm. 613, 121395.
Monteiro, N., Martins, A., Reis, R.L., Neves, N.M., 2014. Liposomes in tissue engineering and regenerative medicine. J. R. Soc. Interface 11, 20140459.
Moore, A., Pinkerton, R., 2009. Vincristine: can its therapeutic index be enhanced? Pediatr. Blood Cancer 53, 1180–1187.
Naseer, F., Ahmad, T., Kousar, K., Kakar, S., Gul, R., Anjum, S., 2022. Formulation of surface-functionalized hyaluronic acid-coated thiolated chitosan nano-formulation for the delivery of vincristine in prostate cancer: a multifunctional targeted drug delivery approach. J. Drug Deliv. Sci. Technol. 74, 103545.
Nazir, H., AlFutaisi, A., Zacharia, M., Elshinawy, M., Mevada, S., Alrawas, A., Khater, D., Jaju, D., Wali, Y., 2017. Vincristine-induced neuropathy in pediatric patients with acute lymphoblastic leukemia in Oman: frequent autonomic and more severe cranial nerve involvement. Pediatr. Blood Cancer 64, e2667.
Noble, C.O., Guo, Z., Hayes, M.E., Marks, J.D., Park, J.W., Benz, C.C., Kirpotin, D.B., Drummond, D.C., 2009. Characterization of highly stable liposomal and immunoliposomal formulations of vincristine and vinblastine. Cancer Chemother. Pharmacol. 64, 741–751.
Oto, E., Vaage, J., Quinn, Y., Newman, M., Engbers, C., Uster, P., Zhu, G., George, Z., 1996. The effect of vincristine–polyanion complexes in STEALTH liposomes on pharmacokinetics, toxicity and anti tumor activity. Cancer Chemother. Pharmacol. 39, 138–142.
Pathak, P., Hess, R., Weiss, M., 2014. Liposomal vincristine for relapsed or refractory Ph-negative acute lymphoblastic leukemia: a review of literature. Therapeut. Adv. Hematol. 5, 18–24.
Pauli, G., Tang, W.-L., Li, S.-D., 2019. Development and characterization of the solvent-assisted active loading technology (SALT) for liposomal loading of poorly water-soluble compounds. Pharmaceutics. 11, 465.
Qiu, L., Jing, N., Jin, Y., 2008. Preparation and in vitro evaluation of liposomal chloroquine diphosphate loaded by a transmembrane pH-gradient method. Int. J. Pharm. 361, 56–63.
Samsonov, A.V., Mihalyov, I., Cohen, F.S., 2001. Characterization of Cholesterol-Sphingomyelin Domains and their Dynamics in Bilayer Membranes. Biophys. J. 81, 1486–1500.
Sarris, A.H., Cabanillas, F., Logan, P.M., Burge, C.T.R., Goldie, J.H., Webb, M.S., 2011. Compositions and Methods for Treating Lymphoma, United States.
Serpico, A.F., Visconti, R., Grieco, D., 2020. Exploiting immune-dependent effects of microtubule-targeting agents to improve efficacy and tolerability of cancer treatment. Cell Death Dis. 11, 361.
Silverman, J.A., Deitcher, S.R., 2013. Marqibo® (vincristine sulfate liposome injection) improves the pharmacokinetics and pharmacodynamics of vincristine. Cancer Chemother. Pharmacol. 71, 555–564.
Slotte, J.P., 2016. The importance of hydrogen bonding in sphingomyelin's membrane interactions with co-lipids. Biochim. et Biophys. Acta (BBA) – Biomembr. 1858, 304–310.
Suter, W., Brennard, J., McMillan, S., Fox, M., 1980. Relative mutagenicity of antineoplastic drugs and other alkylating agents in V79 chinese hamster cells, independence of cytotoxic and mutagenic responses. Mutat. Res./Fundament. Mol. Mechan. Mutagen. 73, 171–181.
Torchilin, V.P., 2005. Recent advances with liposomes as pharmaceutical carriers. Nat. Rev. Drug Discov. 4, 145–160.
Wang, E.S., Schiller, G.J., Heffner, L.T., Stock, W., Rao, A.V., Roboz, G.J., Westervelt, P., Wieduwilt, M.J., Yang, J., Prasad, L., Segarini, K., Goldberg, S.L., 2015. Plasma Vincristine Levels are 100-Fold higher with Marqibo® (Vincristine Sulfate LIPOSOME Injection) in place of Standard Vincristine in Combination Chemotherapy of patients ≥ 60 years Old with newly Diagnosed Acute Lymphoblastic Leukemia (ALL). Blood 126, 2491.
Webb, M.S., Bally, M.B., Mayer, L.D., 1996. Sphingosomes for Enhanced Drug Delivery, United States.
Wenxue, M., Fan, W., Robert, J., Weigen, L., Jianxin, W., 2019. Development of a stable single-vial liposomal formulation for vincristine. Int. J. Nanomedicine 14, 4461–4474.
Zhigaltsev, I.V., Maurer, N., Akhong, Q.-F., Leone, R., Leng, E., Wang, J., Semple, S.C., Cullis, P.R., 2005. Liposome-encapsulated vincristine, vinblastine and vinorelbine: a comparative study of drug loading and retention. J. Control. Release 104, 103–111.